

# Targeting chromosomally unstable tumors with a selective KIF18A inhibitor

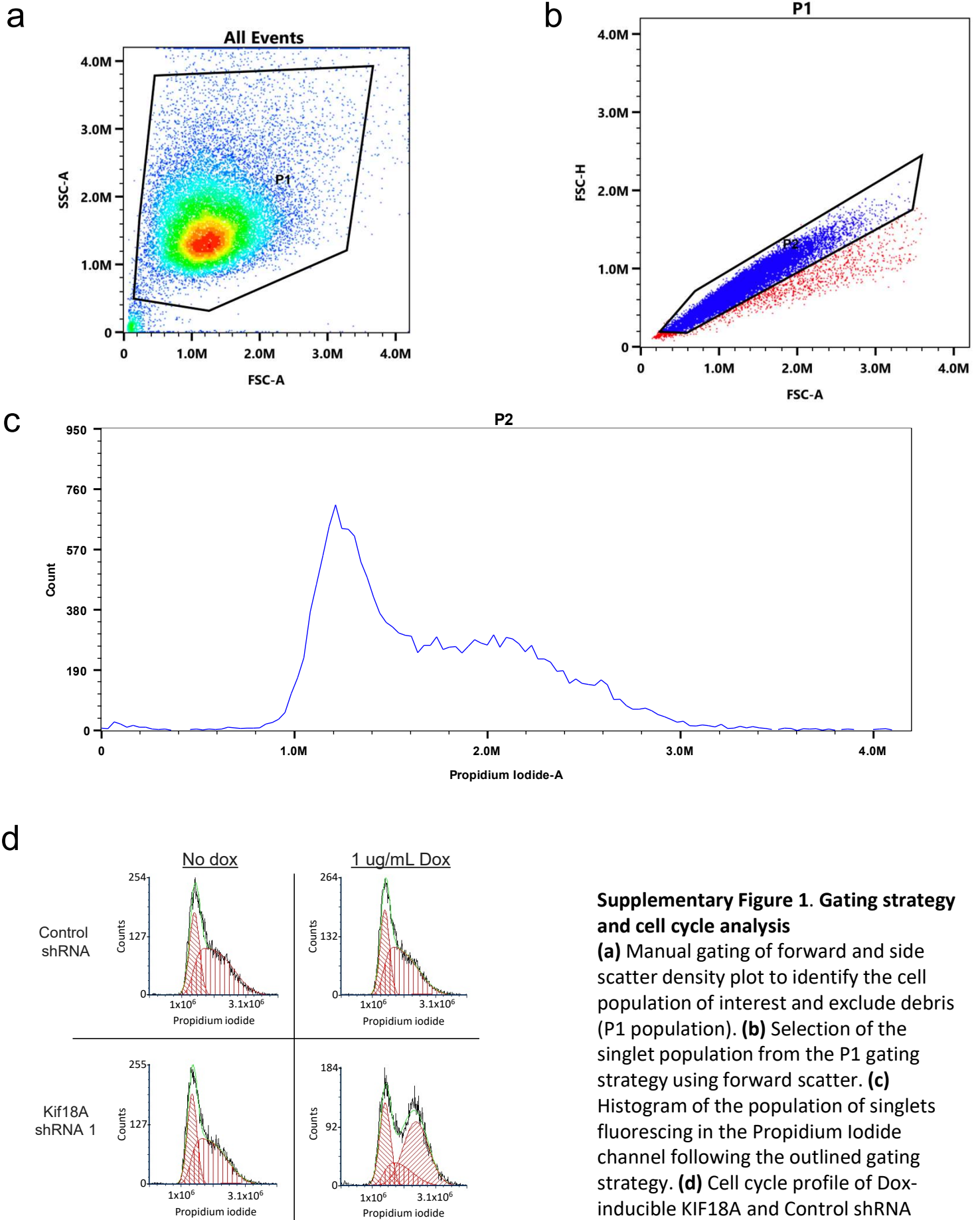
Aaron F. Phillips<sup>1</sup>, Rumin Zhang<sup>1</sup>, Mia Jaffe<sup>1</sup>, Ryan Schulz<sup>1</sup>, Marysol Chu Carty<sup>1</sup>, Akanksha Verma<sup>1</sup>, Tamar Y. Feinberg<sup>1</sup>, Michael D. Arensman<sup>1</sup>, Alan Chiu<sup>1</sup>, Reka Letso<sup>1</sup>, Nazario Bosco<sup>1</sup>, Katelyn A. Queen<sup>2</sup>, Allison R. Racela<sup>2</sup>, Jason Stumpff<sup>2</sup>, Celia Andreu-Agullo<sup>1</sup>, Sarah E. Bettigole<sup>1</sup>, Rafael S. Depetris<sup>1</sup>, Scott Drutman<sup>1</sup>, Shinsan M. Su<sup>1</sup>, Derek A. Cogan<sup>1</sup>, Christina H. Eng<sup>1\*</sup>

<sup>1</sup>*Volastra Therapeutics, 1361 Amsterdam Ave., Suite 520, New York, NY 10027, U.S.A.*

<sup>2</sup>*Department of Molecular Physiology and Biophysics, University of Vermont, Burlington, VT*

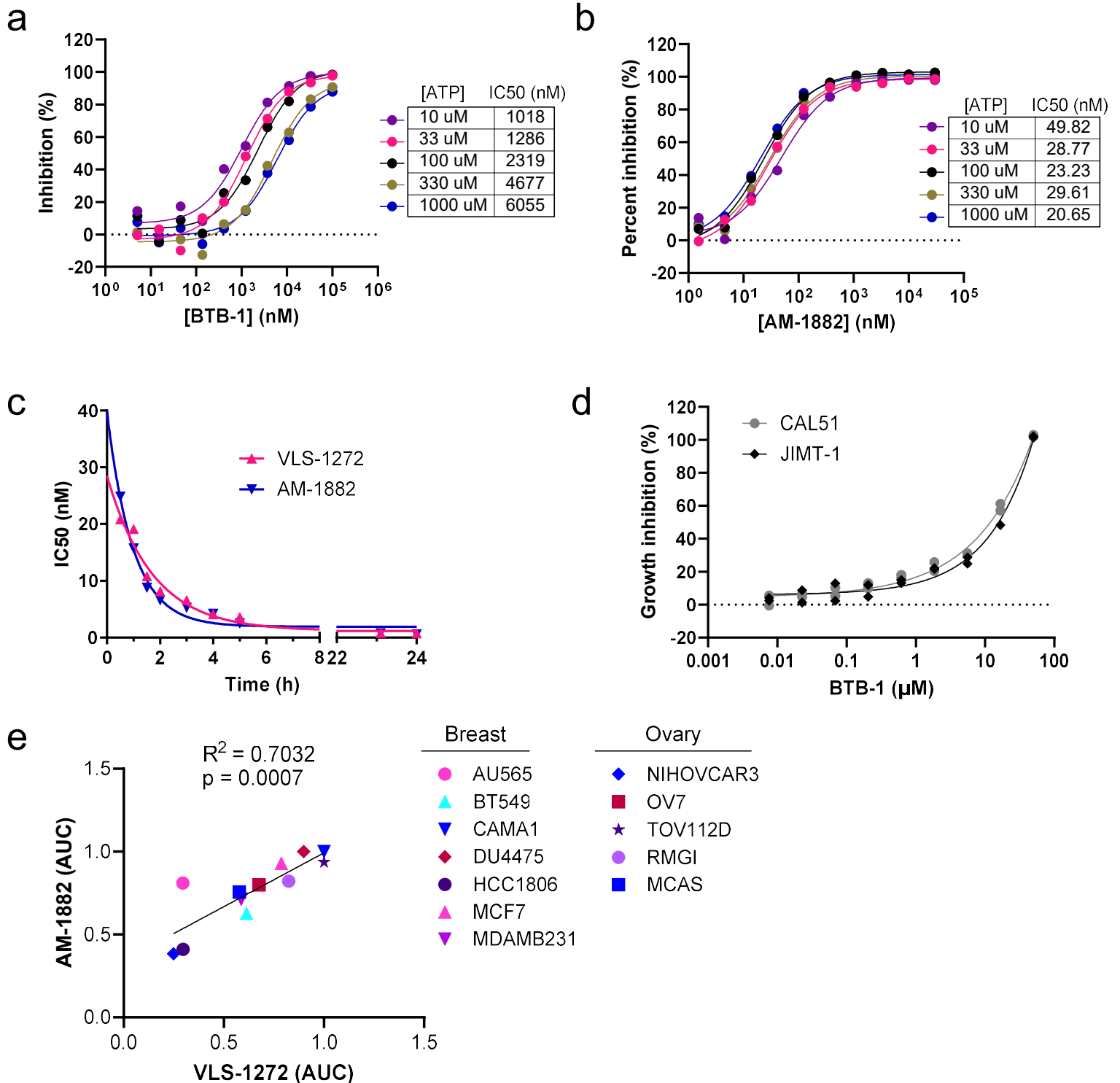
*\*correspondence: ceng@volastratx.com*

## Supplementary Information



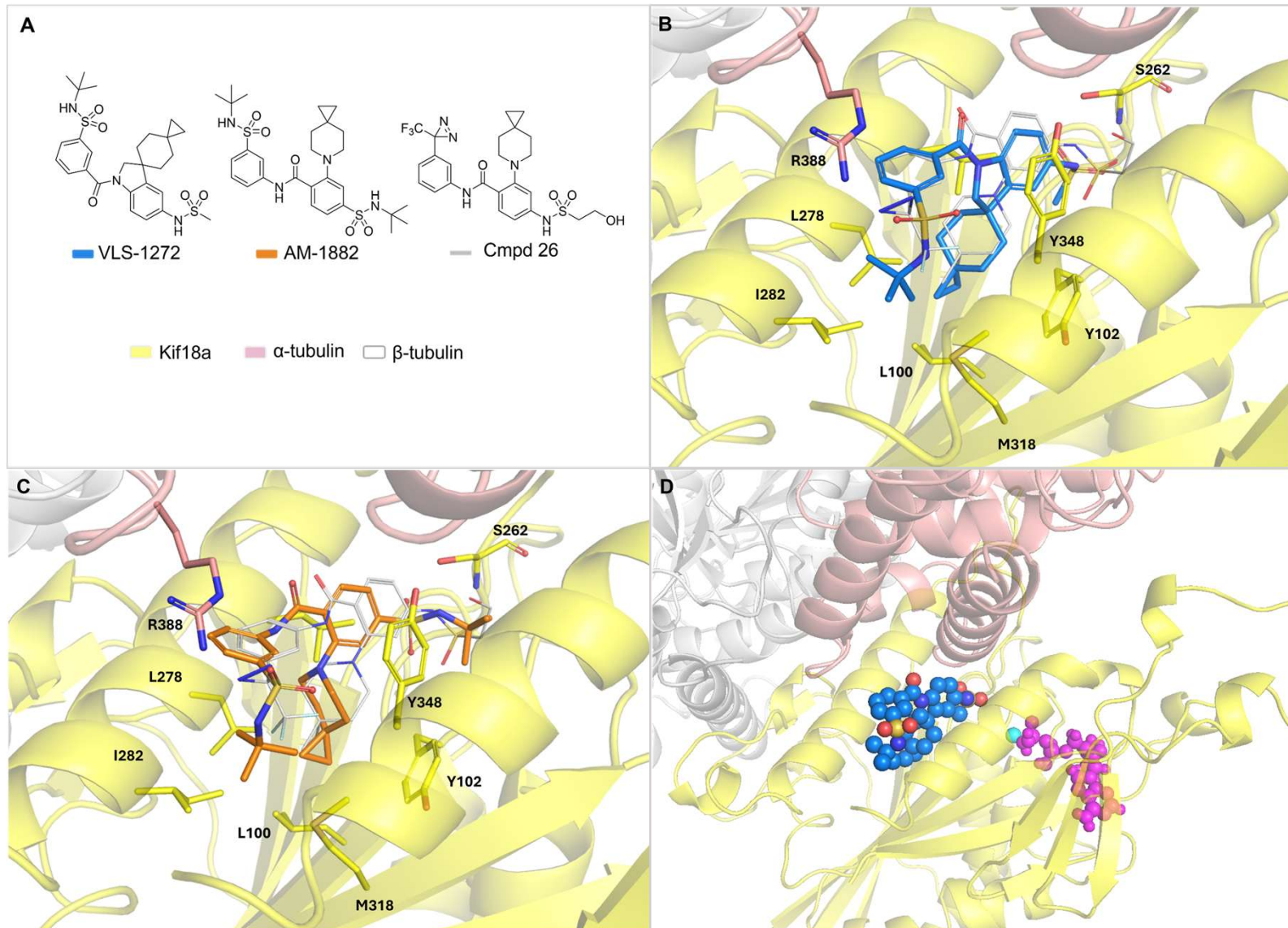
### Supplementary Figure 1. Gating strategy and cell cycle analysis

**(a)** Manual gating of forward and side scatter density plot to identify the cell population of interest and exclude debris (P1 population). **(b)** Selection of the singlet population from the P1 gating strategy using forward scatter. **(c)** Histogram of the population of singlets fluorescing in the Propidium Iodide channel following the outlined gating strategy. **(d)** Cell cycle profile of Dox-inducible KIF18A and Control shRNA JIMT-1 cells after 72h Dox treatment.



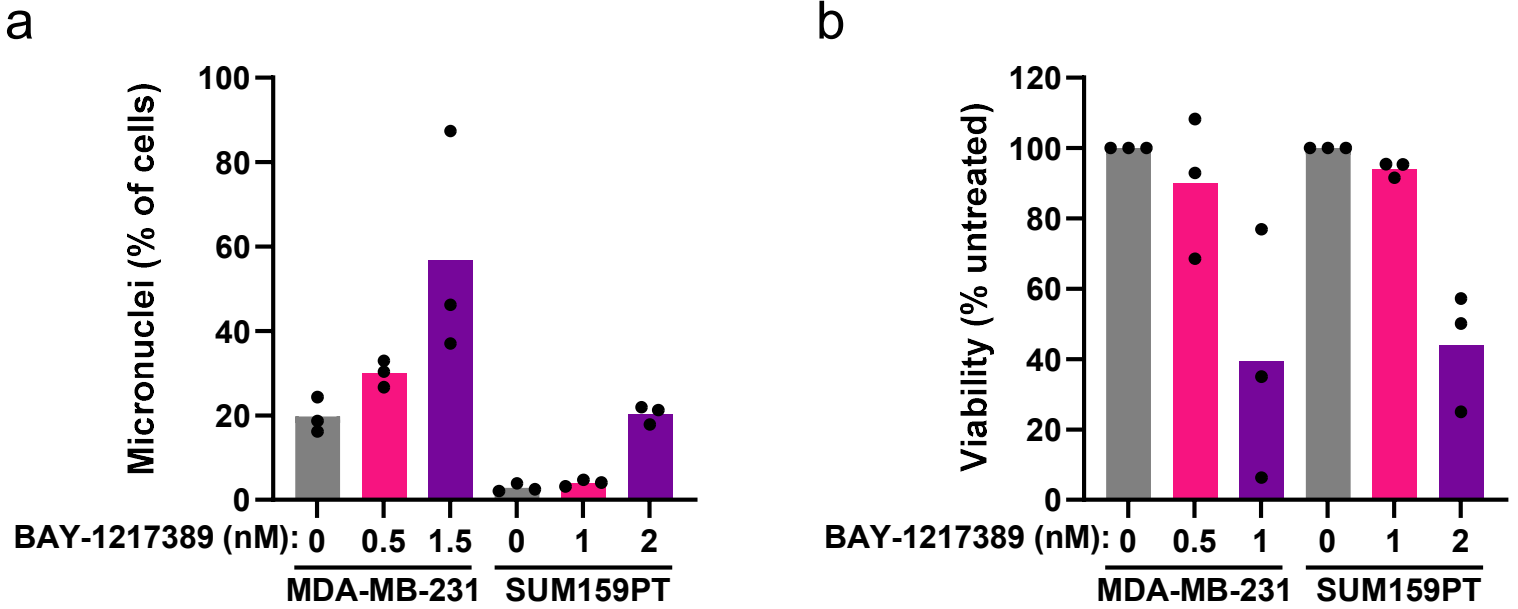
### Supplementary Figure 2. Comparison of VLS-1272 to BTB-1 and AM-1882

**(a)** Potency of BTB-1 in a KIF18A (1-374) biochemical ADP-Glo assay to measure ATPase activity with varied concentrations of ATP. Data presented as mean values from  $n=2$  biological replicates. **(b)** Potency of AM-1882 in a KIF18A (1-374) biochemical ADP-Glo assay to measure ATPase activity with varied concentrations of ATP. Data presented as mean values from  $n=2$  biological replicates. **(c)** IC<sub>50</sub> of VLS-1272 or AM-1882 plotted vs. incubation time of ATPase assay. Data presented as mean values from  $n=2$  biological replicates. **(d)** Growth inhibition measured by CellTiter-Glo of CAL51 (CIN<sup>Low</sup>) and JIMT-1 (CIN<sup>High</sup>) cell lines after treatment with BTB-1 for 168 hours. Data presented as individual values from  $n=2$  biological replicates. **(e)** AUC values of VLS-1272 plotted against published AUC values of AM-1882<sup>36</sup>. Source data are provided in the Source Data file.



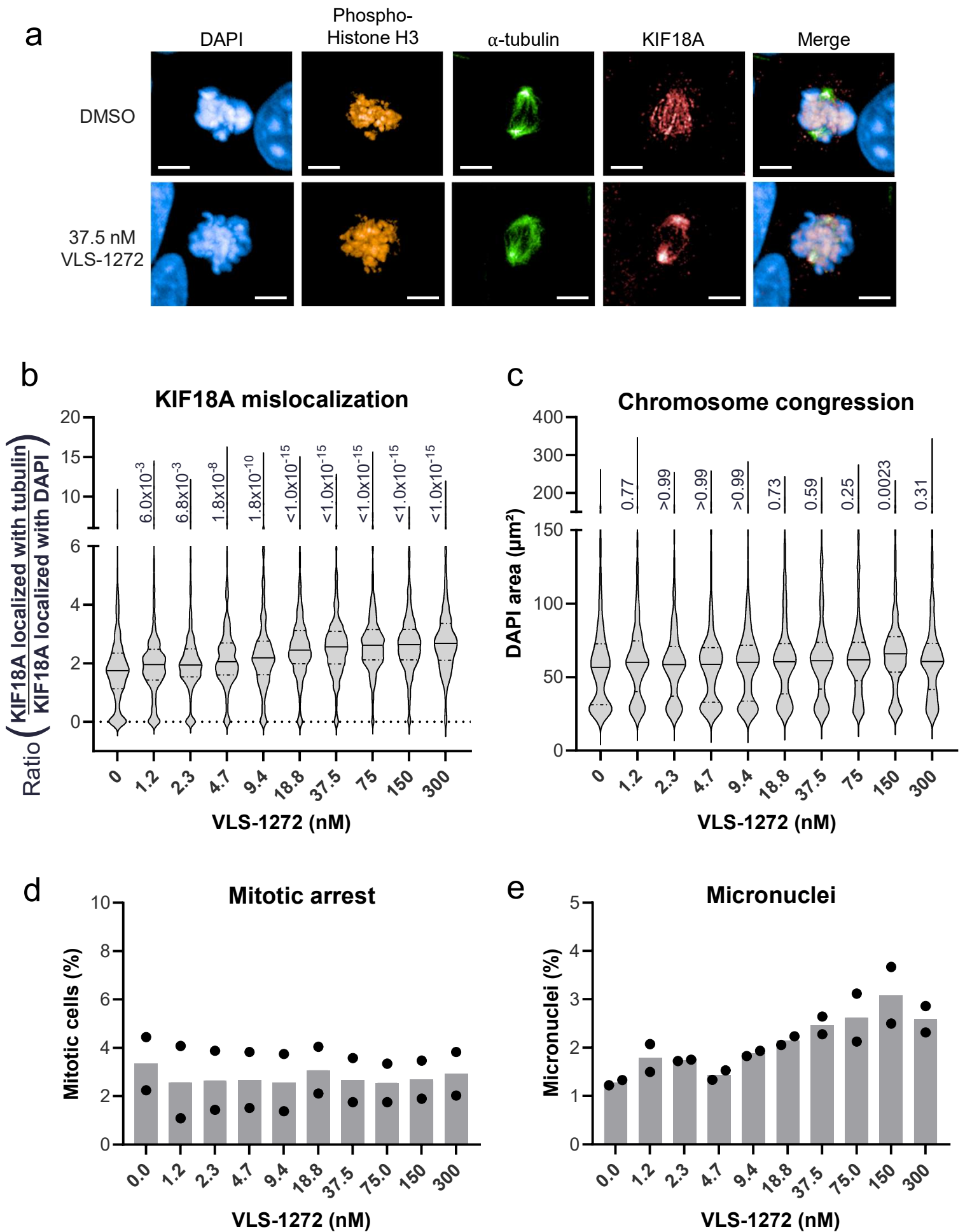
**Supplementary Figure 3: Modelling of KIF18A inhibitors bound in allosteric site at interface of KIF18A and  $\alpha$ -tubulin from docking to homology model of KIF18A,  $\alpha$ -tubulin, and  $\beta$ -tubulin**

**(a)** Structures of ligands and key for coloring of ligands and proteins in images. **(b-c)** Docking pose of VLS-1272 (b, blue cylinders) and AM-1882 (c, orange cylinders) in the allosteric site overlaid with published pose<sup>40</sup> of Cmpd 26 (gray sticks). **(d)** VLS-1272 (blue) docking pose in homology model together with ADP (purple) from X-ray co-crystal structure (PDB: 3LRE) showing location of allosteric site relative to active site.



#### Supplementary Figure 4. Inhibition of the SAC by MPS1i

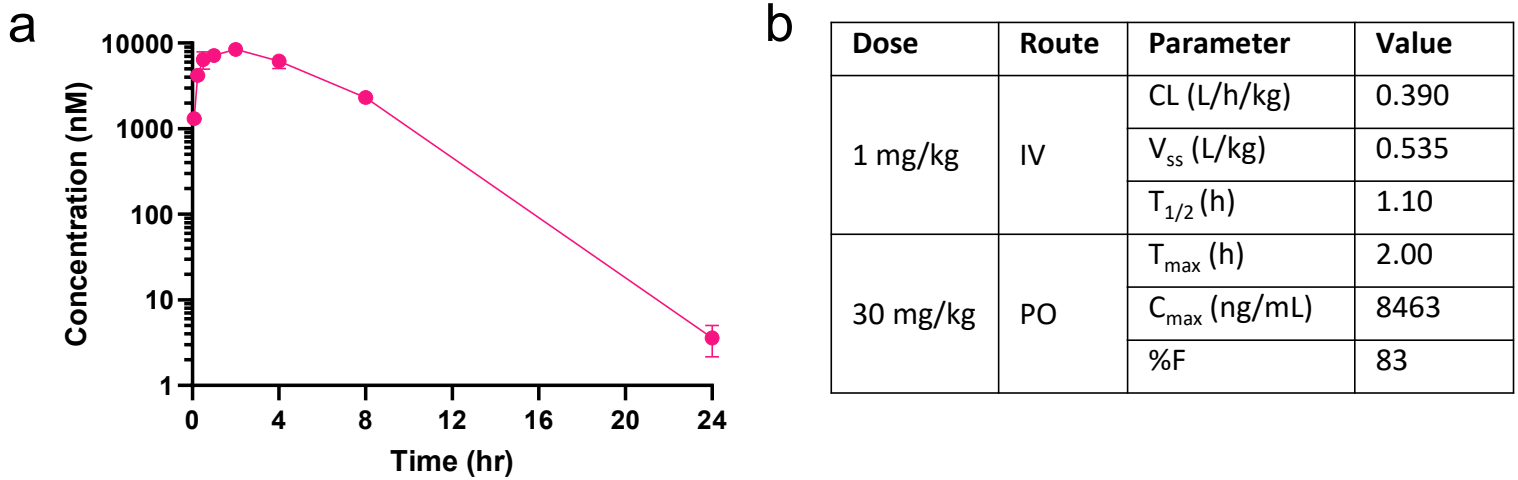
**(a, b)** Cells were treated with the indicated doses of the MPS1 inhibitor BAY-1217389 for 5 days (MDA-MB-231) or 7 days (SUM159PT). Cells were quantified for micronuclei (a) as calculated by the percentage of total micronuclei over total primary nuclei, or viability (b) calculated as a percentage of treated cells to untreated control. Data presented as mean values from n=3 biological replicates. Source data are provided in the Source Data file.



### Supplementary Figure 5. Mitotic consequences of KIF18A inhibition in CAL51 cells with VLS-1272

**(a)** Immunofluorescence images of mitotic CAL51 cells treated with DMSO (top) or 37.5 nM VLS-1272 (bottom). Scale bar = 5  $\mu\text{m}$ . One representative image from the treatment and control group from two biological replicates is shown. **(b)** Quantification of KIF18A mis-localization in mitotic CAL51 cells measured as the ratio of KIF18A colocalizing with the  $\alpha$ -tubulin spindle to KIF18A colocalizing with DNA (DAPI). Colocalization masks were generated in Harmony high-content analysis software. Data presented as violin plots with the mean (solid line) and quartiles (dashed lines) from  $n = 497$ - $582$  mitotic cells. Adjusted p value is calculated compared to untreated control and labeled next to each condition, using one-way ANOVA with Bonferroni's multiple comparisons test. **(c)** Quantification of the area of DAPI staining ( $\mu\text{m}^2$ ) in mitotic cells treated with increasing doses of VLS-1272. The area of the DAPI-stained DNA was calculated in Harmony high-content analysis software. Data presented as violin plots with the mean (solid line) and quartiles (dashed lines) from  $n = 506$ - $590$  mitotic cells. Adjusted p value is calculated compared to untreated control and labeled next to each condition, using one-way ANOVA with Bonferroni's multiple comparisons test. **(d)** Quantification of mitotic CAL51 cells identified by positive staining for pHH3 compared to the number of total DAPI stained nuclei. The mitotic cell population was calculated in Harmony high-content analysis software. Data presented as mean values with individual data points shown from  $n=2$  biological replicates. **(e)** Percentage of total micronuclei to primary nuclei in cells treated with VLS-1272, calculated in Harmony high-content analysis software. Data presented as mean values with individual data points shown from  $n=2$  biological replicates. Source data are provided in the Source Data file.





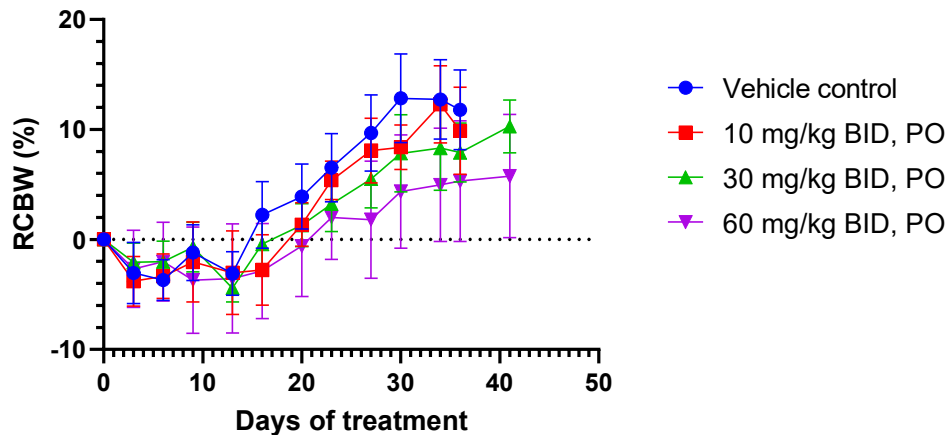
### Supplementary Figure 6. Mean plasma drug concentrations over time

**(a)** Plasma was collected from male CD-1 mice at the indicated times following a single dose of 30 mg/kg VLS-1272-SDD for pharmacokinetic analysis. Data presented as mean plasma concentration of VLS-1272 from  $n=3$  individual mice  $\pm$  standard deviation. **(b)** PK parameters after single IV dose of 1 mg/kg VLS-1272 or single oral gavage of VLS-1272-SDD at 30 mg/kg in male CD-1 mice. Source data are provided in the Source Data file.



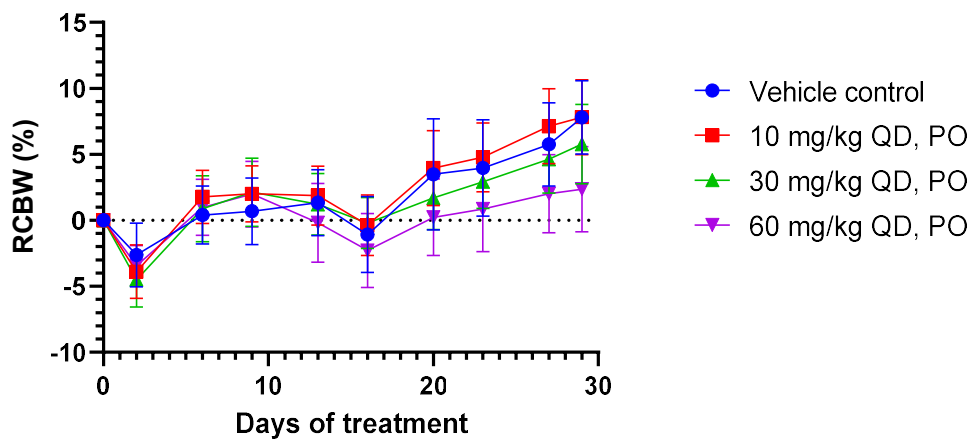
a

## Body weight change in HCC15 CDX model

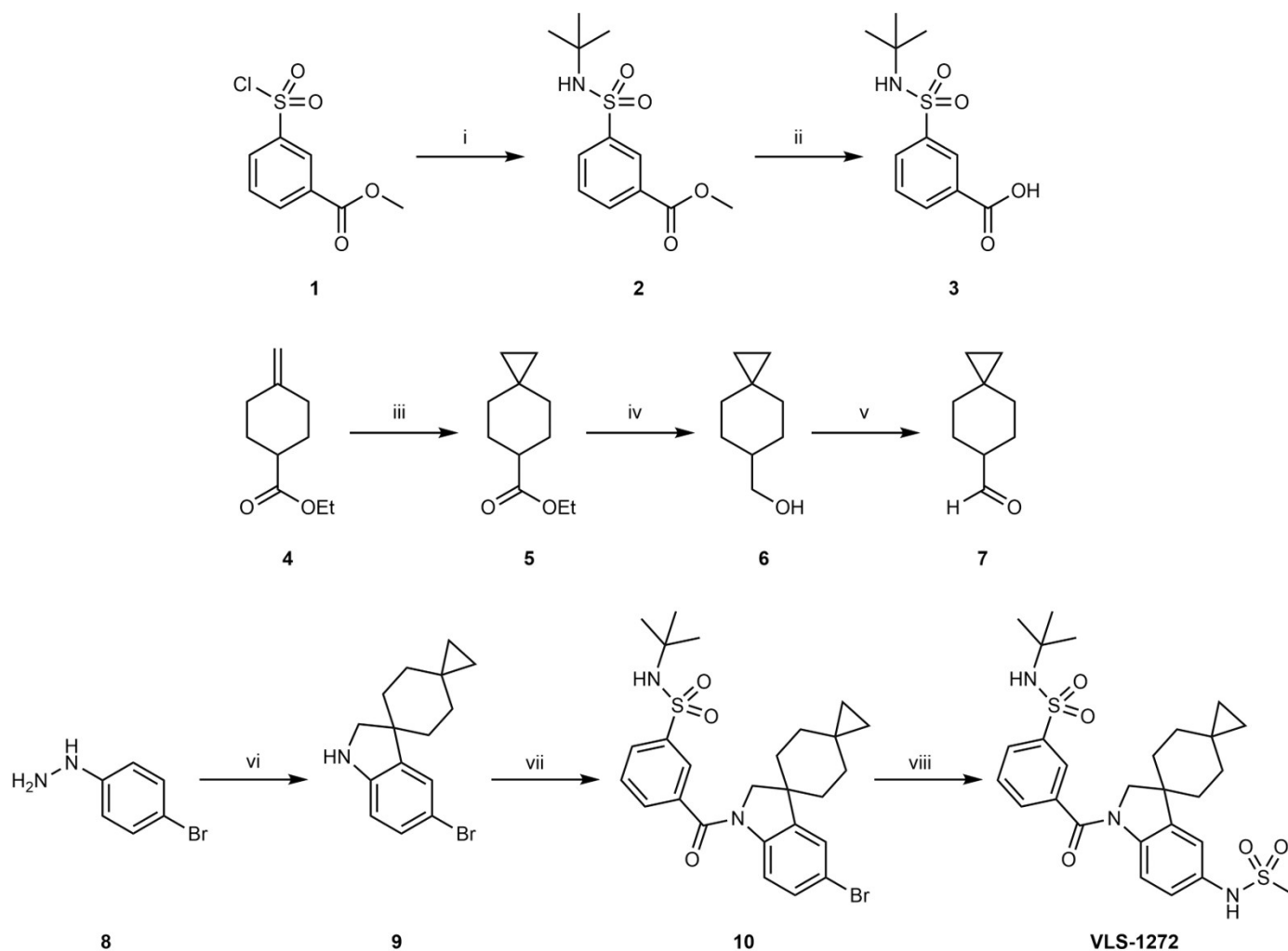


b

## Body weight change in OVCAR3 CDX model

**Supplementary Figure 7. Relative change in body weight from VLS-1272 efficacy studies**

**(a)** Relative change in percent body weight (RCBW) (%) after BID administration of VLS-1272-SDD to female SCID Beige mice bearing HCC15 xenograft tumors (n = 10 mice per treatment group). Nutrient supplements were provided to all groups. BW change was calculated relative to animal weight before the first injection. Data points represent percent group mean change in BW. Error bars represent standard error of the mean (SEM). **(b)** Relative change in percent body weight (RCBW) (%) after QD administration of VLS-1272-SDD to female Balb/c nude mice bearing OVCAR-3 xenograft tumors (n = 10 mice per treatment group). BW change was calculated relative to animal weight before the first injection. Data points represent percent group mean change in BW. Error bars represent standard error of the mean (SEM). Source data are provided in the Source Data file.



### Supplementary Figure 8. Synthesis of VLS-1272

*Reagents and Conditions:* i) t-butylamine,  $i\text{Pr}_2\text{NEt}$ , 96%. ii) LiOH, MeOH,  $\text{H}_2\text{O}$ , 99%. iii)  $\text{Et}_3\text{Zn}$ ,  $\text{CH}_2\text{I}_2$ , TFA, 87%. iv)  $\text{LiAlH}_4$ , 86%. v) PCC. vi) **7**, TFA, 31% (2 steps). vii) HATU,  $i\text{Pr}_2\text{NEt}$ , 53%. viii)  $\text{MeSO}_2\text{NH}_2$ , CuI,  $N^1,N^2$ -dimethylcyclohexane-1,2-diamine, 57%.

Method Info

Instrument: Shimadzu LC-20AD XR MSD:LCMS-2020

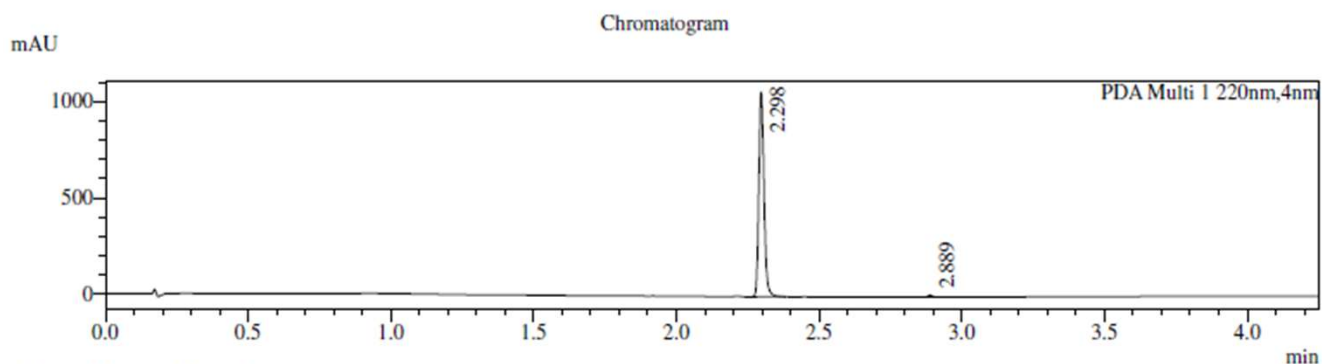
Mobile Phase:A:0.04%TFA in H2O

Mobile Phase:B:0.02%TFA in ACN

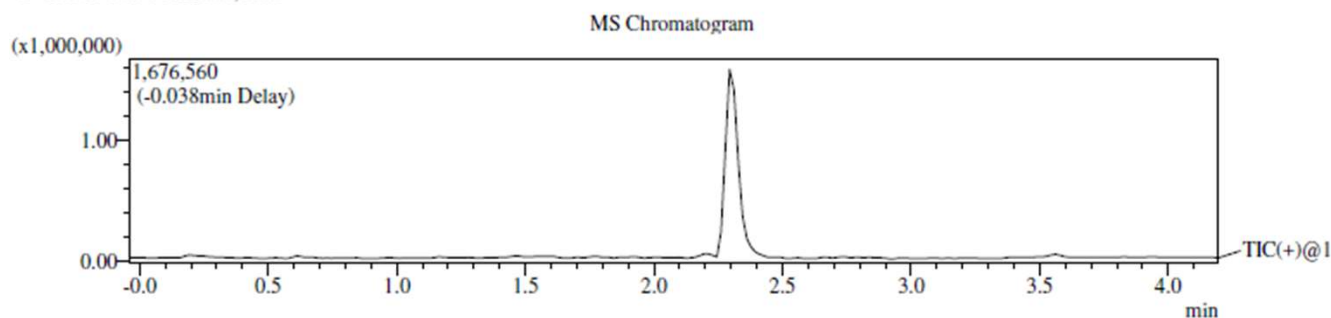
Total Flow : 1.0000 mL/min

Oven Temperature : 40 C

Time	Module	Command	Value	Comment
0.01	Pumps	B.Conc	5	
0.40	Pumps	B.Conc	5	
3.00	Pumps	B.Conc	95	
4.00	Pumps	B.Conc	95	
4.01	Pumps	B.Conc	5	
4.50	Controller	Stop		



1 PDA Multi 1 / 220nm,4nm

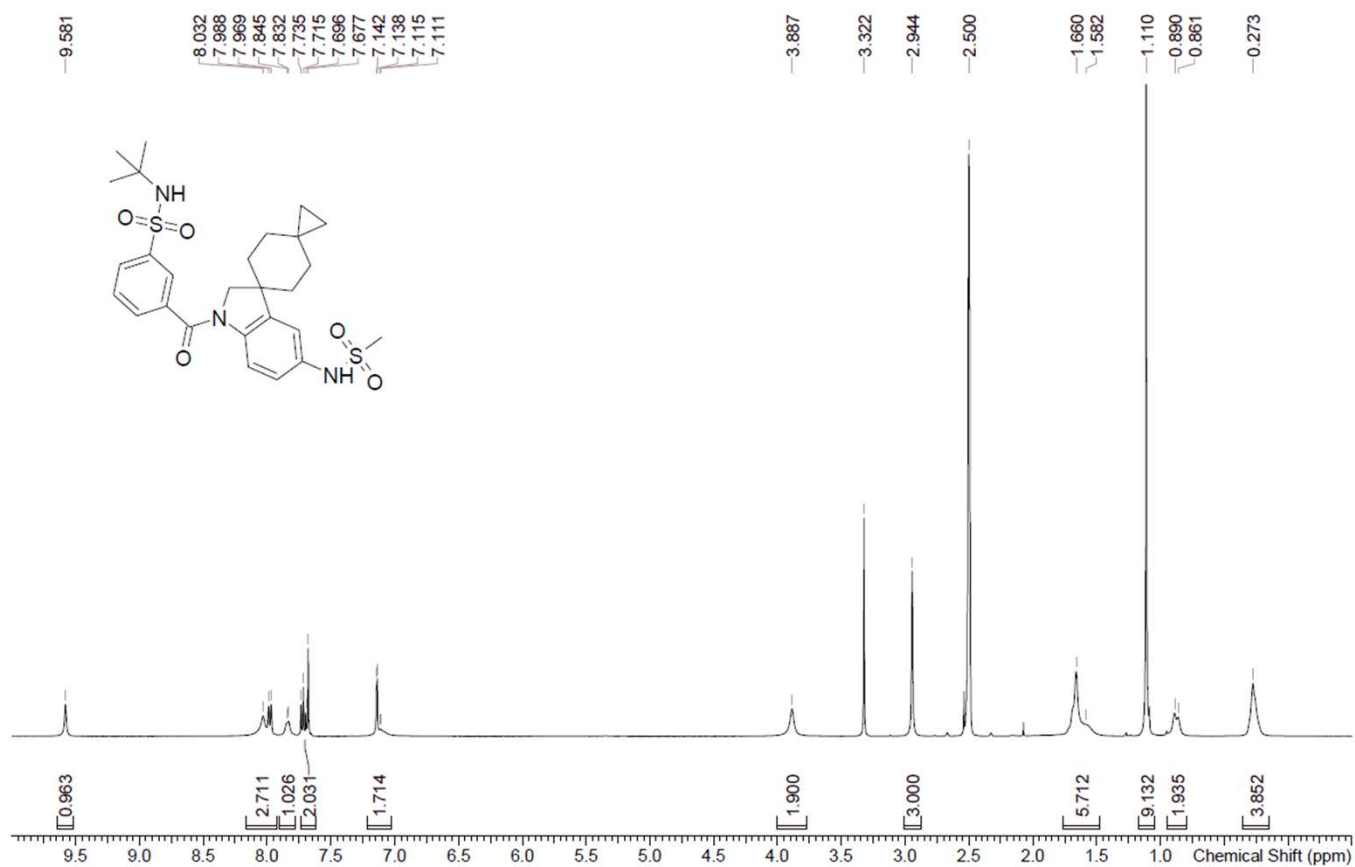


=====  
 Integration Result  
 =====

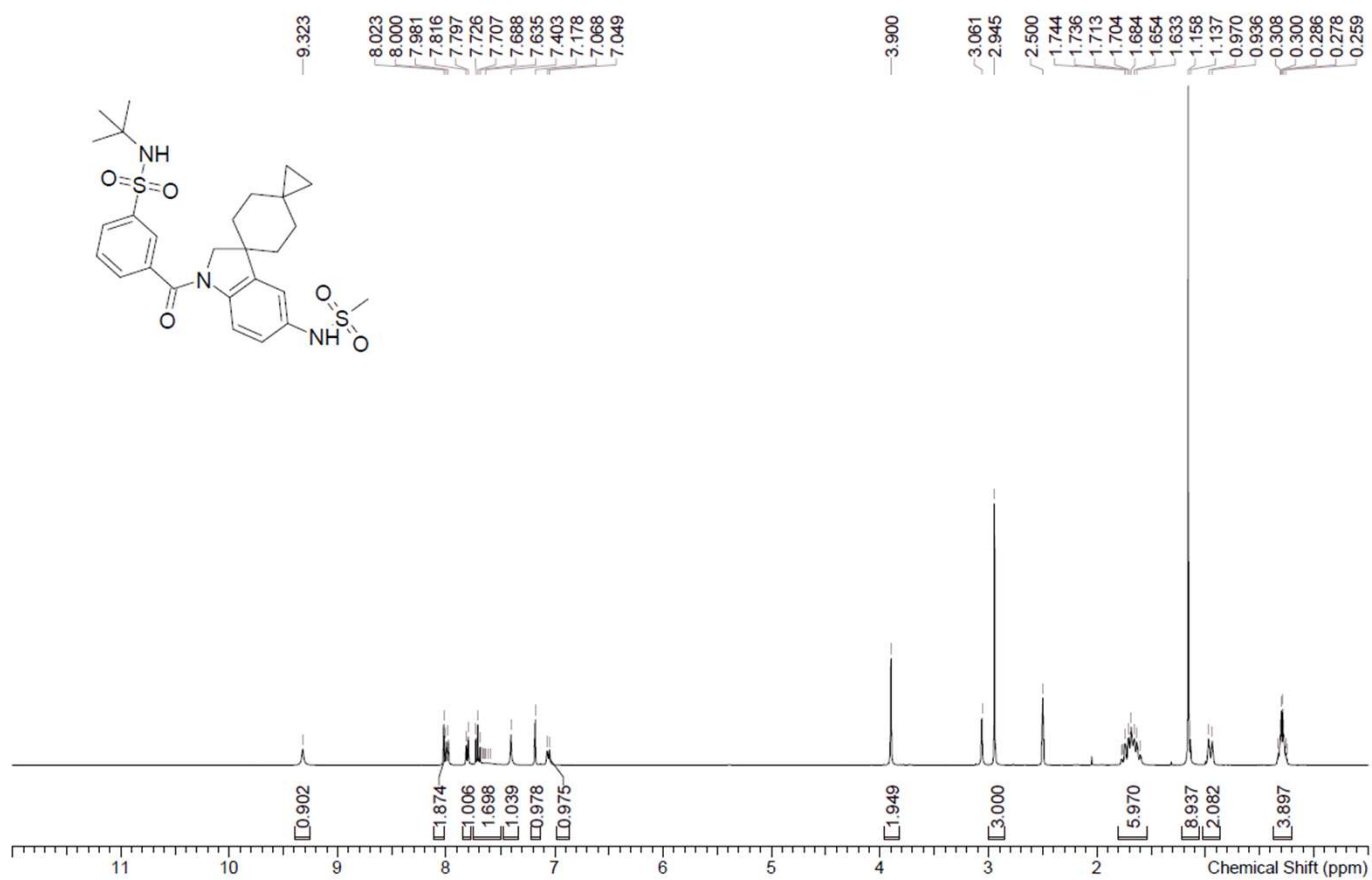
Peak Table

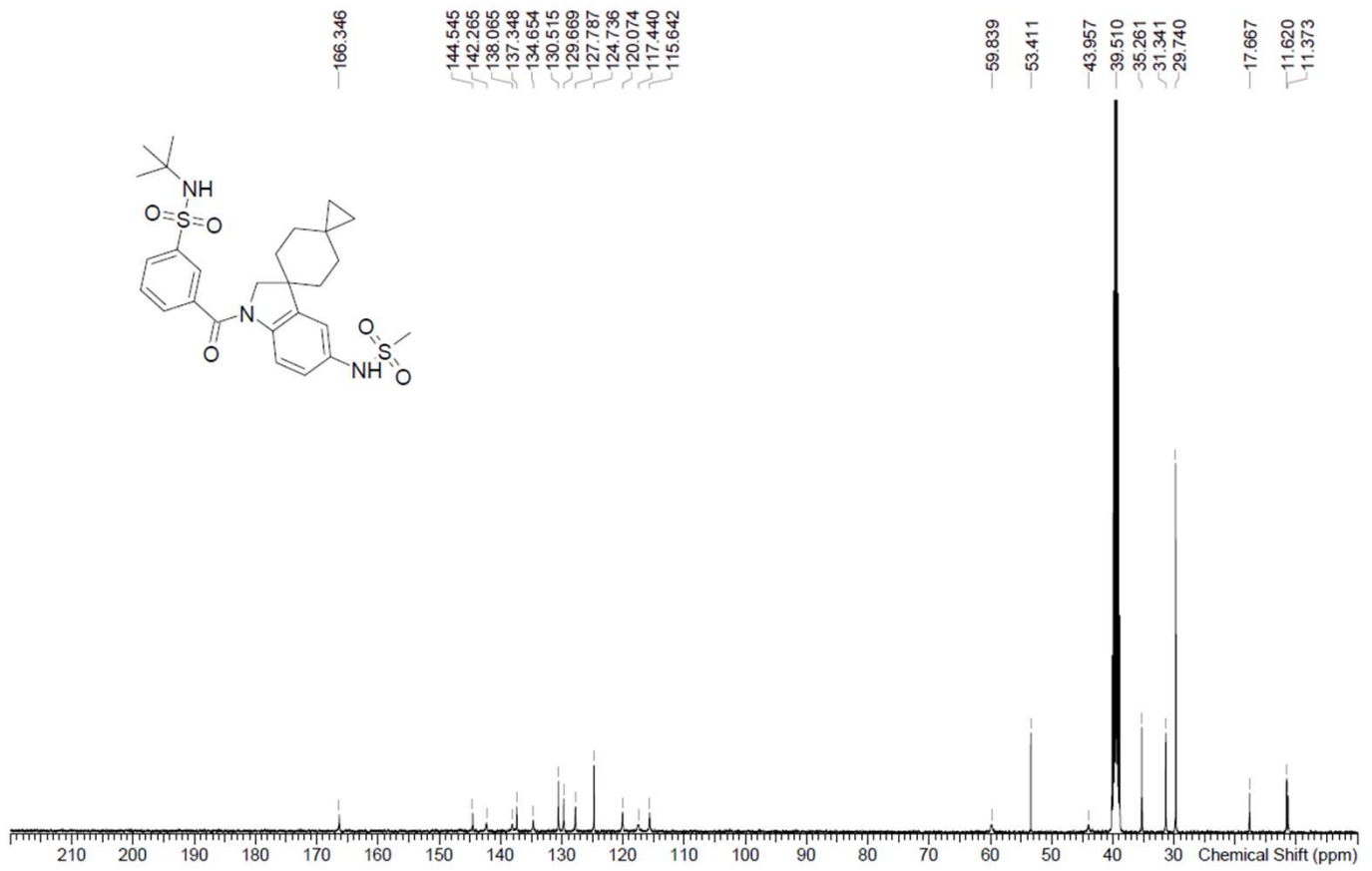
PDA Ch1 220nm						
Peak#	Ret. Time	Height	Height%	USP Width	Area	Area%
1	2.298	1059972	99.052	0.034	1343222	99.098
2	2.889	10143	0.948	0.033	12231	0.902

Supplementary Figure 9. HPLC conditions and trace for VLS-1272 purity determination

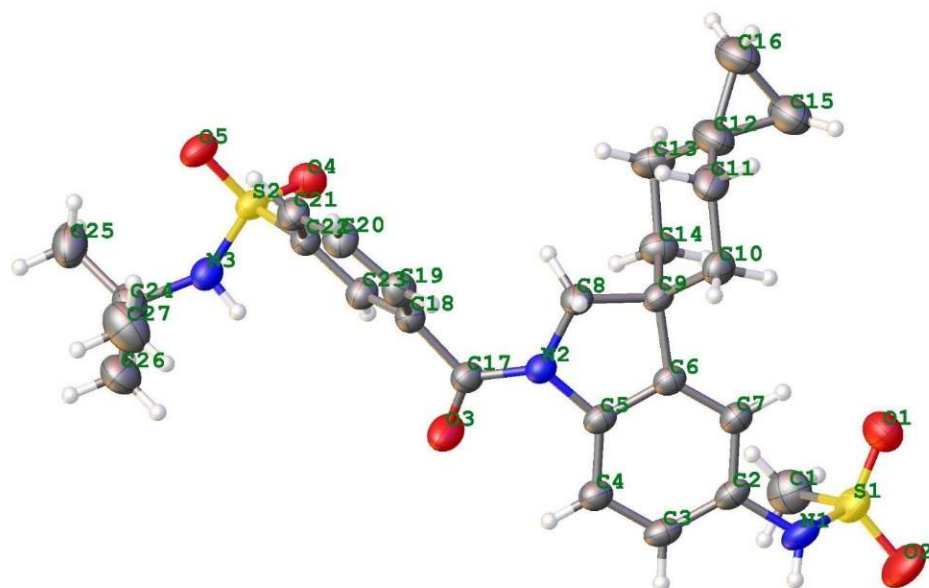


Supplementary Figure 10. <sup>1</sup>H NMR of VLS-1272 at room temperature

Supplementary Figure 11: <sup>1</sup>H NMR of VLS-1272 at 80 °C



Supplementary Figure 12: <sup>13</sup>C NMR of VLS-1272



Supplementary Figure 13: ORTEP plot of VLS-1272



Property	VLS-1272	AM-1882
KIF18A IC <sub>50</sub>	61 ×/÷ 1.2 nM	87 ×/÷ 1.3 nM*
MT-dependence	Requires MT	Requires MT
Time-dependence	Slow-binding	Slow-binding*
ATP-dependence	noncompetitive with ATP	noncompetitive with ATP*
KIF18B IC <sub>50</sub>	>100 μM	> 10 μM
KIF19 IC <sub>50</sub>	0.28 μM (7x)	1.82 μM (8x)
Eg5 IC <sub>50</sub>	>100 μM	>100 μM
KIFC1 IC <sub>50</sub>	>100 μM	>25 μM
Effect on KIF18A spindle localization	Redistributes towards spindle poles	Redistributes towards spindle poles
OVCAR3 IC <sub>50</sub>	11 nM (168 h treatment)	20 nM (96 h treatment)
Primary T cells IC <sub>50</sub>	>3 μM (72h treatment)	0.91 μM (48h treatment)
Effect on mitotic index	Increase in pHH3	Increase in pHH3

### Supplementary Table 1. Comparison of VLS-1272 and AM-1882

Properties of VLS-1272 and AM-1882. Data for VLS-1272 are reported in this study, data for AM-1882 noted by \* were determined in this study, all other properties for AM-1882 were previously published<sup>36</sup>

Dosing group	60 mg/kg, BID x 7 days, PO		30 mg/kg, BID x 7 days, PO	
	<i>Mean</i>	<i>SD</i>	<i>Mean</i>	<i>SD</i>
NEUT# (10 <sup>9</sup> /L)	0.918	0.214	0.886	0.196
LYMPH# (10 <sup>9</sup> /L)	0.126	0.087	0.108	0.041
MONO# (10 <sup>9</sup> /L)	0.080	0.016	0.098	0.033
EO# (10 <sup>9</sup> /L)	0.060	0.046	0.042	0.028
BASO# (10 <sup>9</sup> /L)	0.000	0.000	0.000	0.000
NEUT (%)	77.340	8.193	77.480	7.858
LYMPH (%)	10.700	7.780	9.580	3.286
MONO (%)	6.800	0.917	9.060	4.274
EO%(%)	5.160	4.148	3.880	3.051
BASO (%)	0.000	0.000	0.000	0.000
RBC (10 <sup>12</sup> /L)	9.328	0.833	9.250	0.508
HGB (g/L)	145.600	14.293	144.000	7.036
HCT (%)	41.220	3.748	41.380	1.918
MCV (fL)	44.200	0.682	44.760	0.639
MCH (pg)	15.600	0.245	15.560	0.152
MCHC (g/L)	353.000	4.950	348.000	1.871
RDW-CV (%)	17.900	1.696	18.280	0.642
PLT (10 <sup>9</sup> /L)	1030.000	150.236	1091.400	263.330
MPV (fL)	6.600	0.158	6.700	0.224

**Supplementary Table 2. Hematology from VLS-1272-treated mice**

Complete blood counts from naïve female SCID Beige mice orally dosed with 30 mg/kg or 60 mg/kg VLS-1272-SDD BID for 7 days. Data shown are the mean and standard deviation from 5 mice per group.